

Influence of the stacking sequence on layered-chalcogenides properties: First principle investigation of $\text{Pb}_2\text{Bi}_2\text{Te}_5$

Weiliang MA,^{ab} Marie-Christine RECORD,^{*a} Jing TIAN,^{ab} and Pascal BOULET^b

^a Aix-Marseille University, University of Toulon, CNRS, IM2NP, Marseille, France. E-mail: weiliang.ma@etu.univ-amu.fr,

* Corresponding author: m-c.record@univ-amu.fr

^b Aix-Marseille University, CNRS, MADIREL, Marseille, France. E-mail: jing.tian@etu.univ-amu.fr; pascal.boulet@univ-amu.fr

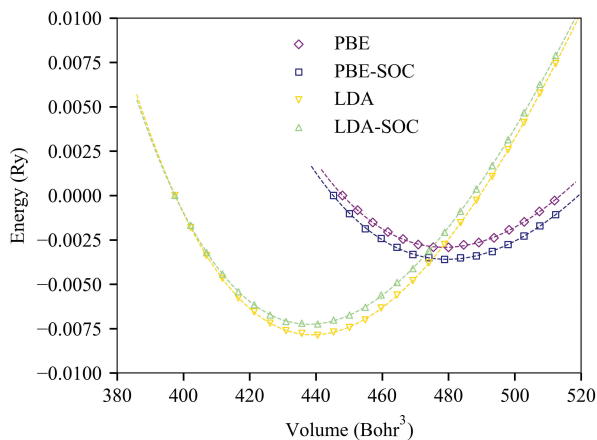


Figure S1 Relative energy versus cell volume for PbTe.

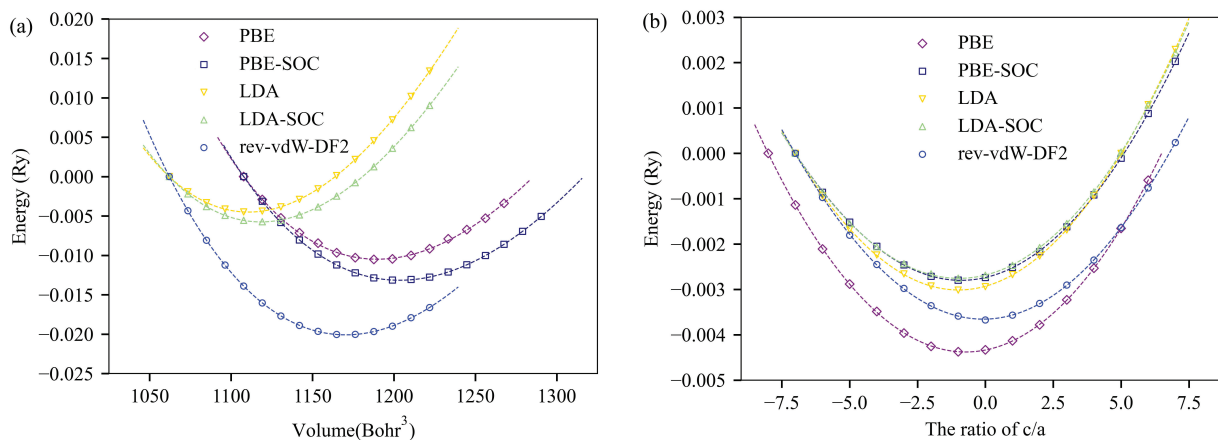


Figure S2 Relative energy versus cell volume (a) and a/c ratio (b) for Bi_2Te_3 .

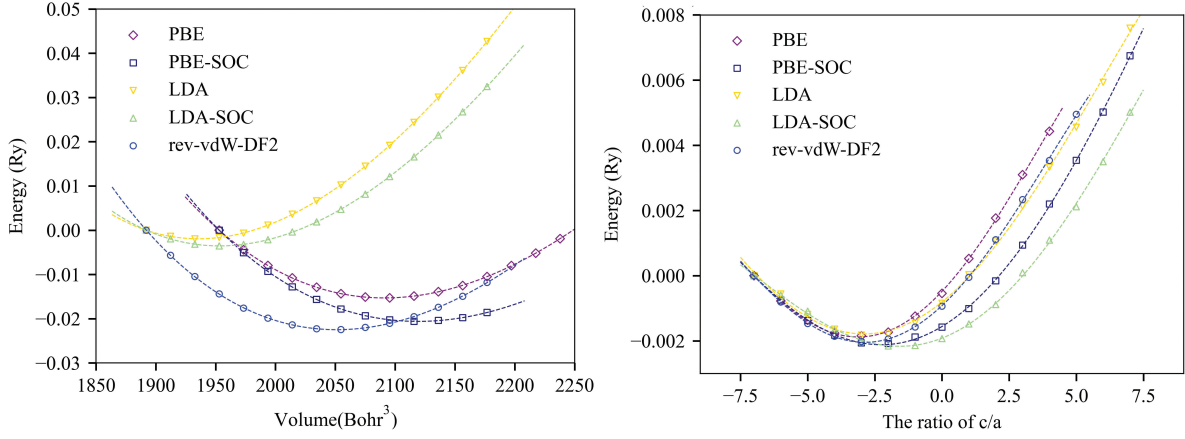


Figure S3 Relative energy versus cell volume (a) and a/c ratio (b) for $\text{Pb}_2\text{Bi}_2\text{Te}_5$ with stacking A.

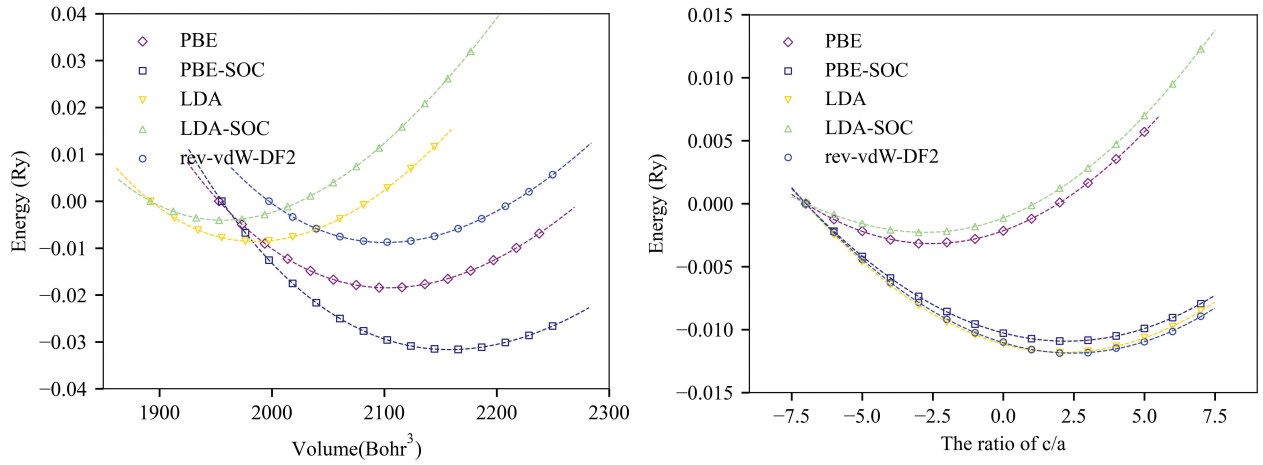


Figure S4 Relative energy versus cell volume (a) and a/c ratio (b) for $\text{Pb}_2\text{Bi}_2\text{Te}_5$ with stacking B.

Table S1 Topological properties of PbTe and Bi_2Te_3 corresponding to the BCPs in Figure S8a,b; r_1 is the distance between BCP and Bi; r_2 is the distance between BCP and Te; r_1 and r_2 are in unit of pm; the angle is between BCPs and their two ends; ρ and $\nabla^2\rho$ are the electron charge density and its Laplacian at the BCPs in unit of $10^{-2}e/\text{bohr}^3$ and $10^{-2}e/\text{bohr}^5$; G , V and H represent the kinetic, potential and total energy densities at the BCPs in unit of $10^{-2}a.u./\text{bohr}^3$.

BCP	r_1	r_2	r_1/r_2	angle	ρ	$\nabla^2\rho$	G	V	H	$ V /G$	H/ρ
PbTe-b	158.2	170.4	0.9286	180.00	2.672	3.111	1.20	-1.63	-0.43	1.35	-1.60
$\text{Bi}_2\text{Te}_3\text{-b1}$	157.5	165.3	0.9526	179.84	3.095	3.168	1.40	-2.02	-0.61	1.44	-1.98
$\text{Bi}_2\text{Te}_3\text{-b2}$	149.2	156.7	0.9526	179.64	4.267	2.710	1.95	-3.22	-1.27	1.65	-2.98
$\text{Bi}_2\text{Te}_3\text{-b3}$	178.0	178.0	1.0000	180.00	1.379	2.075	0.75	-0.88	-0.13	1.18	-0.75

Table S2 Electron charge density ($10^2\rho$ in e/bohr^3) at the bond critical points along the slab for stacking-A-sequence structures with 9 (S1-1) and 21 (S1-2) layers, for stacking-B-sequence structures with 9 (S2-1) and 21 (S2-2) layers and stacking-B-sequence structures with the Bi atom replaced by a Pb one with 9 (S3-1) and 21 (S3-2) layers. The critical point numbered 1 corresponds to the Te-Te bond across the gap between the slabs.

	1	2	3	4	5	6	7	8	9	10	11
S1-1	1.77	4.15	1.99	4.02	3.06						
S2-1	1.38	4.08	2.83	2.90	2.86						
S3-1	1.69	3.60	2.26	2.98	2.67						
S1-2	1.41	4.06	1.71	3.93	2.93	3.04	3.57	2.54	3.58	2.75	3.20
S2-2	1.04	3.94	2.69	2.75	2.70	2.74	2.73	2.74	2.73	2.74	2.74
S3-2	1.70	3.62	2.19	3.02	2.49	2.87	2.61	2.79	2.67	2.75	2.71

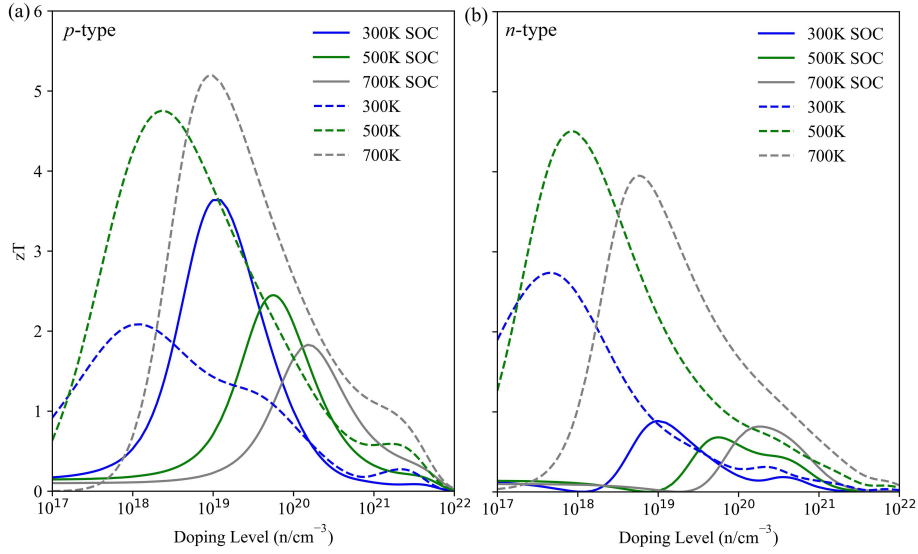


Figure S5 Calculated figure of merit zT of Pb₂Bi₂Te₅ stacking A with p -type (a) and n -type (b). The solid and dash lines represent zT with and without SOC.

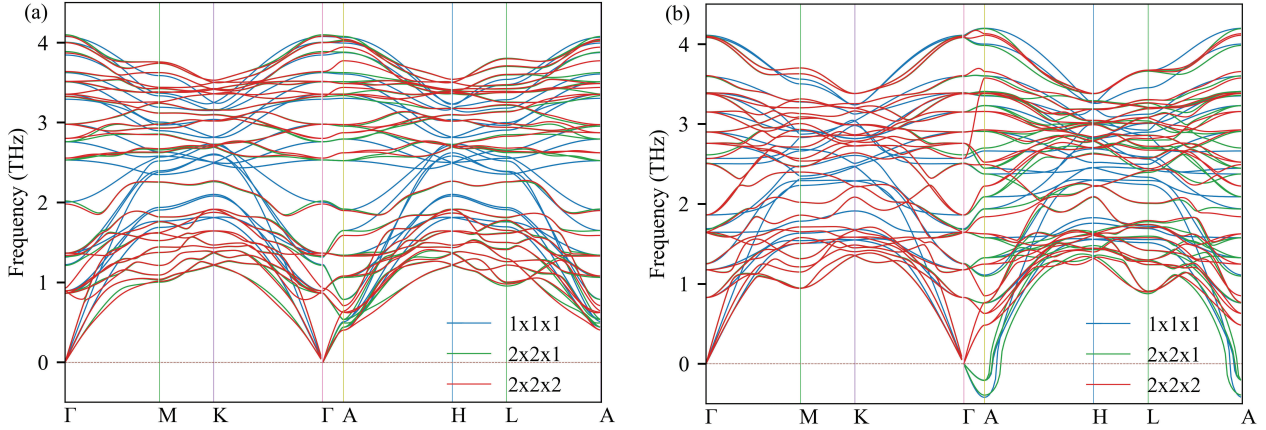


Figure S6 Phonon dispersion convergence of Pb₂Bi₂Te₅ stacking A (a) and stacking B (b) with $1 \times 1 \times 1$, $2 \times 2 \times 1$ and $2 \times 2 \times 2$ supercell.

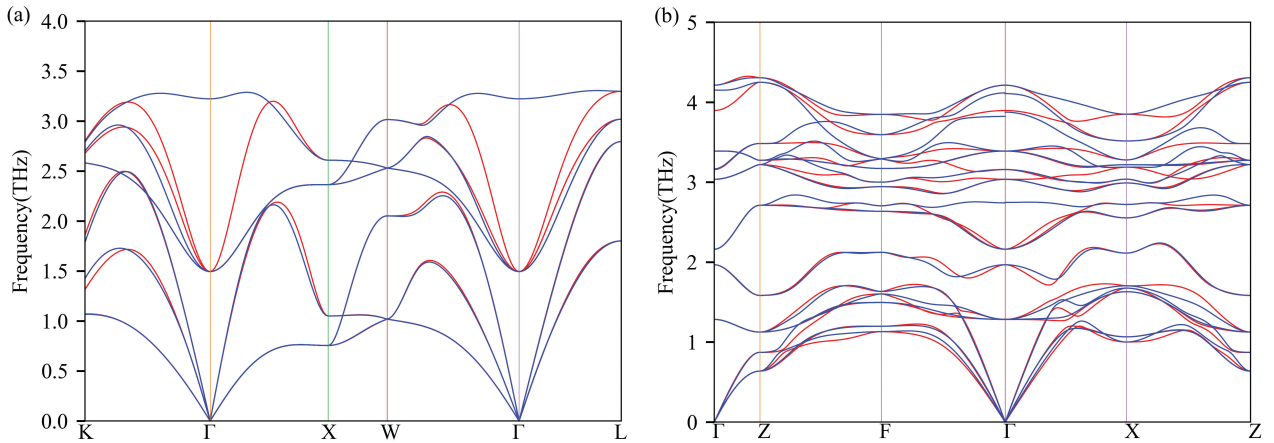


Figure S7 Phonon dispersion of PbTe (a) and Bi₂Te₃ (b) with (blue line) and without (red line) LO-TO splitting effect. Long-range electrostatic interactions are included by evaluating the dielectric tensor and Born effective charges using density functional perturbation theory.

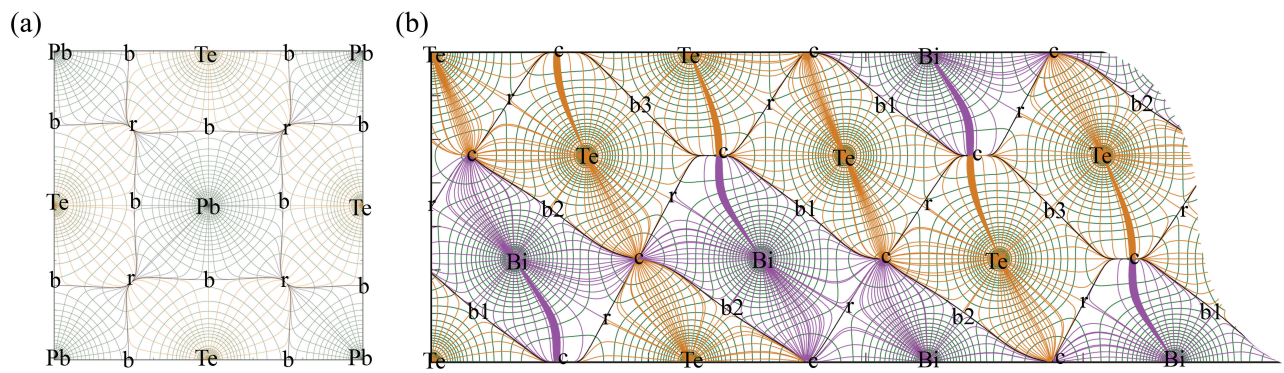


Figure S8 CPs and flux lines derived from $\nabla\rho(r)$ (light green lines) of PbTe (a) in (100)-plane and Bi₂Te₃ (b) in (110)-plane.